

# Crystal Structure and Functional Analysis of the Eukaryotic Class II Release Factor eRF3 from *S. pombe*

Chunguang Kong,<sup>1</sup> Koichi Ito,<sup>2,6</sup> Martin A. Walsh,<sup>3,6</sup> Miki Wada,<sup>2</sup> Yuying Liu,<sup>1</sup> Sundramurthy Kumar,<sup>1</sup> David Barford,<sup>4</sup> Yoshikazu Nakamura,<sup>2</sup> and Haiwei Song<sup>1,5,\*</sup>

<sup>1</sup>Laboratory of Macromolecular Structure  
Institute of Molecular and Cell Biology  
30 Medical Drive  
Singapore 117609

<sup>2</sup>Department of Basic Medical Sciences  
Institute of Medical Science  
University of Tokyo  
4-6-1 Shirokanedai, Minato-ku  
Tokyo 108-8639  
Japan

<sup>3</sup>MRC France  
CRG BM14, ESRF, B.P.220  
F-38043 Grenoble CEDEX  
France

<sup>4</sup>Section of Structural Biology  
Institute of Cancer Research  
237 Fulham Road  
London, SW3 6JB  
United Kingdom

<sup>5</sup>Department of Biological Sciences  
National University of Singapore  
14 Science Drive 4  
Singapore 117543

## Summary

Translation termination in eukaryotes is governed by two interacting release factors, eRF1 and eRF3. The crystal structure of the eEF1 $\alpha$ -like region of eRF3 from *S. pombe* determined in three states (free protein, GDP-, and GTP-bound forms) reveals an overall structure that is similar to EF-Tu, although with quite different domain arrangements. In contrast to EF-Tu, GDP/GTP binding to eRF3c does not induce dramatic conformational changes, and Mg<sup>2+</sup> is not required for GDP binding to eRF3c. Mg<sup>2+</sup> at higher concentration accelerates GDP release, suggesting a novel mechanism for nucleotide exchange on eRF3 from that of other GTPases. Mapping sequence conservation onto the molecular surface, combined with mutagenesis analysis, identified the eRF1 binding region, and revealed an essential function for the C terminus of eRF3. The N-terminal extension, rich in acidic amino acids, blocks the proposed eRF1 binding site, potentially regulating eRF1 binding to eRF3 in a competitive manner.

## Introduction

Translation termination of protein biosynthesis is governed by two major components: the mRNA stop codon at the ribosome A site and the polypeptide chain release

factors (RFs) (reviewed in Kisselev et al., 2003; Nakamura and Ito, 2003; Nakamura et al., 2000). In eukaryotes, translation termination is mediated by two interacting release factors, eRF1 and eRF3, which act as class I and II factors, respectively (Frolova et al., 1994; Stansfield et al., 1995; Zhouravleva et al., 1995). eRF1 functions as an omnipotent release factor, decoding all three stop codons and triggering the release of the nascent peptide catalyzed by the ribosome (Frolova et al., 1994). eRF3 is a GTPase, which enhances the termination efficiency by stimulating the eRF1 activity in a GTP-dependent manner (Stansfield et al., 1995; Zhouravleva et al., 1995). Although eRF1 is the functional equivalent of prokaryotic RF1 and RF2, its tertiary structure is distinct from the crystal structure of bacterial RF2 (Song et al., 2000; Vestergaard et al., 2001). However, when bound to the ribosome, and in the presence of its cognate stop codon, RF2 adopts a conformation that is dramatically different from that of its crystal structure, resembling that of eRF1, suggesting that both the bacterial and eukaryotic class I factors act in a similar way (Rawat et al., 2003; Klaholz et al., 2003). Comparison of eRF3 with its prokaryotic counterpart RF3 shows that they share essential similarities but have some significant differences as well (Kisselev et al., 2003; Nakamura and Ito, 2003; Kisselev and Buckingham, 2000). Sequence comparison of class II release factors with elongation factors shows that RF3 is more similar to EF-G whereas eRF3 is more similar to eEF1 $\alpha$ , implying their precise function may differ (Kisselev and Buckingham, 2000; Nakamura et al., 2000). The mechanism by which RF3 recycles RF1 and RF2 has been clarified, and the mode of action of RF3 has been proposed to be similar to that of EF-Tu, although they carry out quite opposite tasks (Zavialov et al., 2001). Furthermore, the findings that the GTPase activities of eRF3 and RF3 on ribosomes are stimulated by their respective class I factors suggest that both eRF3 and RF3 function in a similar way (Frolova et al., 1996; Zavialov et al., 2001).

On the basis of sequence analysis and functional properties, eRF3 is divided into at least two regions: an amino-terminal nonhomologous region and a conserved C-terminal eEF1 $\alpha$ -like region (reviewed by Kisselev and Buckingham, 2000). The C-terminal region is responsible for translation termination activity and is essential for viability (Zhouravleva et al., 1995; Ter-Avanesyan et al., 1993), while the N-terminal region is dispensable for the termination process but seems to be important for binding poly (A) binding protein (PABP) (Hoshino et al., 1999; Inge-Vechtsov et al., 2003; Uchida et al., 2002). The interaction of the N terminus of eRF3 with PABP is evolutionarily conserved, and such interactions appear to link the termination event with the initiation process in protein biosynthesis (Inge-Vechtsov et al., 2003; Hoshino et al., 1999). Moreover, three functional domains of eRF3 (Sup35p) in *S. cerevisiae* have been defined as N and M, in addition to the C-terminal eEF1 $\alpha$ -like domain. Interestingly, the N domain is responsible for its prion-like [PSI<sup>+</sup>] factor formation, and is rich in glutamine residues (reviewed by Serio and Lindquist, 2000; Cher-

\*Correspondence: haiwei@imcb.a-star.edu.sg

<sup>6</sup>These authors contributed equally to this work.

Table 1. Data Collection, Phase Determination, and Refinement Statistics

	Se-Met MAD Data		eRF3c-GDP	eRF3c-GTP
	$\lambda 1$ (peak)	$\lambda 2$ (remote)		
Wavelength (Å)	0.9788	0.8856	0.9724	0.9724
Resolution (Å)	2.35	2.67	2.7	3.0
Unique reflections (N)	25217	17393	16917	11985
Completeness (%)	99.5(99.5)	99.4(99.4)	100.0(100.0)	98.3(98.3)
Redundancy	6.9	10.7	7.0	7.1
$I/\sigma(I)$	11.2(2.0)	5.6(1.7)	7.8(0.6)	5.2(0.7)
$R_{\text{merge}}^a$ (%)	4.7	8.4	8.6	14.0
Phasing power <sup>b</sup>				
Iso (centric/acentric)	1.11/1.35			
Ano	2.20	1.1		
Number of sites	13			
Figure of merit				
Before density modification	0.42			
After density modification	0.84			
Refinement Statistics	eRF3c	eRF3c-GDP	eRF3c-GTP	
Resolution range (Å)	20-2.35	20-2.9	20-3.2	
Reflection used	23902	12967	9417	
$R_{\text{cryst}}^c$	25.5	25.6	26.6	
$R_{\text{free}}^d$	28.4	28.4	31.9	
Nonhydrogen atoms				
Protein (N)	6466	6451	6466	
Nucleotide (N)		28	32	
Waters (N)	178	75	58	
R.m.s. deviations				
Bond length (Å)	0.013	0.011	0.012	
Bond angle (°)	1.3	1.3	1.4	

Values in parentheses indicate the specific values in the highest resolution shell.

<sup>a</sup>  $R_{\text{merge}} = \sum |I_i - \langle I \rangle| / \sum I_i$ , where  $I_i$  is the intensity of an individual reflection, and  $\langle I \rangle$  is the average intensity of that reflection.

<sup>b</sup> Phasing power = rms ( $|F_H|/E$ ), where ( $|F_H|$ ) = heavy atom structure factor amplitude, and  $E$  = residual lack of closure.

<sup>c</sup>  $R_{\text{cryst}} = \sum ||F_o| - |F_c|| / \sum |F_o|$ , where  $F_o$  denotes the observed structure factor amplitude, and  $F_c$  denotes the structure factor amplitude calculated from the model.

<sup>d</sup>  $R_{\text{free}}$  is as for  $R_{\text{cryst}}$  but calculated with 10% of randomly chosen reflections omitted from the refinement.

noff et al., 2002). In mammals, two eRF3 variants designated as eRF3a (GSPT1) and eRF3b (GSPT2) having a long nonhomologous stretch at their N termini have been identified (Hoshino et al., 1989, 1998).

The eEF1 $\alpha$ -like C-terminal region of eRF3 can be further divided into the GTP binding domain resembling those found in RF3, EF-G, EF-Tu, and eEF1 $\alpha$ , and the C-terminal domain that is involved in interaction with eRF1 (reviewed by Kisselev et al., 2003; Kisselev and Buckingham, 2000). Yeast two-hybrid deletion analysis indicated that the C-terminal domains of eRF3 and eRF1 mediated their complex formation whereas their GTPase domains were dispensable for such interactions (Merkulova et al., 1999; Frolova et al., 2000; Ito et al., 1998; Ebihara and Nakamura, 1999). In addition to interactions with eRF1, eRF3 interacts via its eEF1 $\alpha$ -like region with Upf1p, Upf2p, and Upf3p, proteins of the RNA surveillance complex that mediate nonsense-mediated mRNA decay (NMD), and these interactions appear to influence translation termination efficiency (Czapinski et al., 1999; Wang et al., 2001).

As a first step toward understanding the molecular mechanism of the class II release factor in translation termination, we have determined the crystal structure of the C-terminal eEF1 $\alpha$ -like region of eRF3 from *S. pombe* in three states: free, GDP-, and GTP-bound

forms. These results, the first structure of a class II release factor to be defined, reveal a three-domain architecture that resembles those of eEF1 $\alpha$  and EF-Tu. However, our study reveals novel features for guanine nucleotide binding and the exchange mechanism of eRF3. The interaction site with eRF1 has been identified on the molecular surface and analyzed by mutagenesis.

## Results and Discussion

### Structure Determination

The structure of the N-terminal truncated *S. pombe* eRF3 (residues 196-662, corresponding to the eEF1 $\alpha$  homology region), designated as eRF3c, was determined using the MAD method. The current model has been refined at a resolution of 2.35 Å to working and free R factors of 25.5% and 28.4%, respectively. No bound nucleotide was found in this structure. Attempts to cocrystallize eRF3c with either GDP or GDPNP failed. Therefore, crystals of eRF3c were soaked in a buffer containing either GDP or GDPNP. The structures of eRF3c in complex with either GDP (eRF3c-GDP) or GDPNP (eRF3c-GTP) were solved by the molecular replacement method. Difference Fourier maps clearly showed the bound nucleotides but without bound Mg<sup>2+</sup> ion despite the presence of 2 mM Mg<sup>2+</sup> in the soaking

buffer. The electron densities of the phosphate moieties for both GDP and GDPNP are well defined while the density for the guanine base of GDPNP is less well defined than those of GDP. In all three structures, three regions of polypeptide are not visible in the electron density map and are assumed to be disordered, namely residues 196-214, 280-307, and 325-335. Statistics of structure determination and refinement are summarized in Table 1 (see Experimental Procedures).

### Overall Structure

The polypeptide chain of eRF3c is folded into three domains with overall dimensions of  $41 \text{ \AA} \times 49 \text{ \AA} \times 82 \text{ \AA}$  (Figure 1A). Domain 1 (residues 237-467) represents the GTPase domain that binds the guanine nucleotide, and in common with other GTPases such as EF-Tu and Ras, is composed of a six-stranded  $\beta$  sheet of mixed polarity (five parallel and one antiparallel  $\beta$  strand) flanked by six  $\alpha$  helices and a single  $3_{10}$  helix. Domain 1 is connected to domain 2 (residues 468-554) by a long stretch of peptide with a single helical turn in the middle. Domain 2 is connected to domain 3 (residues 555-662) by a short extended stretch of peptide. Both domains 2 and 3 form a  $\beta$  barrel structure as observed in EF-Tu and eEF1 $\alpha$  (Kjeldgaard and Nyborg, 1992; Song et al., 1999; Andersen et al., 2000a;b). The N-terminal extension (residues 215-236), corresponding to part of the middle domain of *S. cerevisiae* eRF3 (Figure 3A), is situated in between domains 2 and 3, contacting one end of each of their respective  $\beta$  barrels. There are no interdomain contacts between domains 1 and 2, and domains 1 and 3, whereas domain 1 interacts with domain 3 in both GDP- and GTP-bound EF-Tu structures (Kjeldgaard and Nyborg, 1992; Song et al., 1999; Berchtold et al., 1993). The overall structures of all three domains are similar to one another among all three of our crystal structures (free form, GDP-, and GTP-bound form; mean pair-wise  $C_{\alpha}$  r.m.s.d.  $\sim 0.6 \text{ \AA}$ ) with the exception of a single variable region (residues 245-249) corresponding to part of the P loop.

### Comparison of eRF3c with EF-Tu and eEF1 $\alpha$

Figure 1 illustrates the structures of eRF3c, EF-Tu-GDP (Song et al., 1999), the EF-Tu-GTP-tRNA ternary complex (Nissen et al., 1995), and eEF1 $\alpha$  of the eEF1 $\alpha$ -eEF1 $\beta$  binary complex (Andersen et al., 2000a). The individual domain structures are similar among these proteins. Superposition of domain 1 of eRF3c with those of EF-Tu-GDP and eEF1 $\alpha$  gives an r.m.s.d. for equivalent  $C_{\alpha}$  atoms of 1.5  $\text{\AA}$  and 1.3  $\text{\AA}$ , respectively. When domains 2 and 3 are superimposed, the r.m.s.d. for  $C_{\alpha}$  atoms is 1.6  $\text{\AA}$  and 1.5  $\text{\AA}$  for eRF3c versus EF-Tu-GDP and eRF3c vs eEF1 $\alpha$ , respectively. Despite these similarities, the relative orientation of domain 1 with respect to domains 2 and 3 in eRF3c is quite different from those in both EF-Tu-GDP and eEF1 $\alpha$ . When domain 1 of eRF3c is superimposed with that of EF-Tu-GDP, the orientations of domains 2 and 3 differ by  $144^{\circ}$  (Figure 2A). Similar results are obtained when the corresponding domains of eRF3c and eEF1 $\alpha$  (Andersen et al., 2000a) are compared with each other (Figures 2B).

Apart from the differences in their relative domain orientations, there are local structural changes as well.

Part of the switch I region in eRF3c (residues 267-276) folds into an  $\alpha$  helix (Figure 1A), corresponding to the single turn  $\alpha$  helix of switch I in EF-Tu-GDP (Figure 1D), and the first helix of the switch I region of eEF1 $\alpha$  in complex with eEF1 $\beta$  (Figure 1B). The orientation of this helix in eRF3c is rotated by  $104^{\circ}$  relative to the corresponding helix of switch I in eEF1 $\alpha$  (Figure 2B). The rest of switch I in eRF3c, which contains the conserved metal binding residue Thr303 (Thr61 of EF-Tu), is disordered. The switch II region, which contributes an Asp residue for  $Mg^{2+}$  coordination in all the GTPases (Asp322 of eRF3, Asp80 of EF-Tu), consists of G2, an extended peptide segment plus a helical structure in both EF-Tu-GDP and eEF1 $\alpha$  (Figures 1B and 1D) (Kjeldgaard and Nyborg, 1992; Song et al., 1999; Berchtold et al., 1993). Surprisingly, the  $\alpha$ -helix of switch II is completely disordered in eRF3c. Importantly, disorder of the switch I and II regions is not caused by crystal packing as these regions are distant from any symmetry-related molecule. Asp322 of switch II displays a markedly different conformation from its counterpart in EF-Tu (Figure 3B; see below). Such structural differences may profoundly affect nucleotide and  $Mg^{2+}$  binding to eRF3c.

### Guanine Nucleotide Binding to eRF3c

Amino acids involved in nucleotide recognition are largely restricted to four loops connecting secondary structural elements (G1/P loop, G2, G3, and G4; Figure 3B). The guanine base is held in a hydrophobic pocket between a methylene group of Lys385 from G3 and Tyr429 from G4 (Figures 4A to 4C). The interactions of the guanine moiety and the ribose ring with the protein residues are very similar to those seen in EF-Tu and eEF1 $\alpha$  (Kjeldgaard and Nyborg, 1992; Song et al., 1999; Andersen et al., 2001). The P loop, defined by the consensus sequence GXXXXGK(S/T), is important for phosphate binding in GTPases (Kjeldgaard and Nyborg, 1992; Kjeldgaard et al., 1996). Upon GDP/GTP binding to eRF3c, residues 245-249 of the P loop undergo a dramatic conformational change to accommodate the bound nucleotide, and surround the  $\beta$ -phosphate group in a semicircular manner (Figure 4A).  $Mg^{2+}$  is an essential cofactor for GTP hydrolysis in all G proteins (Kjeldgaard et al., 1996). In the structures of eRF3c-GDP and eRF3c-GTP, Asp322 of switch II (G2) is too remote from the  $Mg^{2+}$  binding site to coordinate the ion (Figures 4A and 4B). The region of switch I containing Asp292 and Thr303 (corresponding to Asp50 and Thr61 of EF-Tu, respectively) is disordered. Residues Asp50 and Asp80 coordinate the  $Mg^{2+}$  through water molecules in all states of the EF-Tu structure while Thr61 coordinates a  $Mg^{2+}$  ion in the EF-Tu-GTP structure (Song et al., 1999; Berchtold et al., 1993). Not surprisingly,  $Mg^{2+}$  is not present in both eRF3c-GDP and eRF3c-GTP structures due to the disorder of Asp292 and Thr303 in switch I, and the displacement of Asp322. Interestingly, a similar displacement of Asp90 (Asp322 of eRF3) from the nucleotide binding site of *S. solfataricus* EF1 $\alpha$  (SsEF1 $\alpha$ ) accounts for the absence of the  $Mg^{2+}$  in a EF1 $\alpha$ -GDP complex (Vitagliano et al., 2001) (Figure 4C), indicating that eRF3 and SsEF1 $\alpha$  have similar nucleotide binding features.

The finding that  $Mg^{2+}$  has only a marginal effect on nucleotide exchange, but is essential for the GTPase

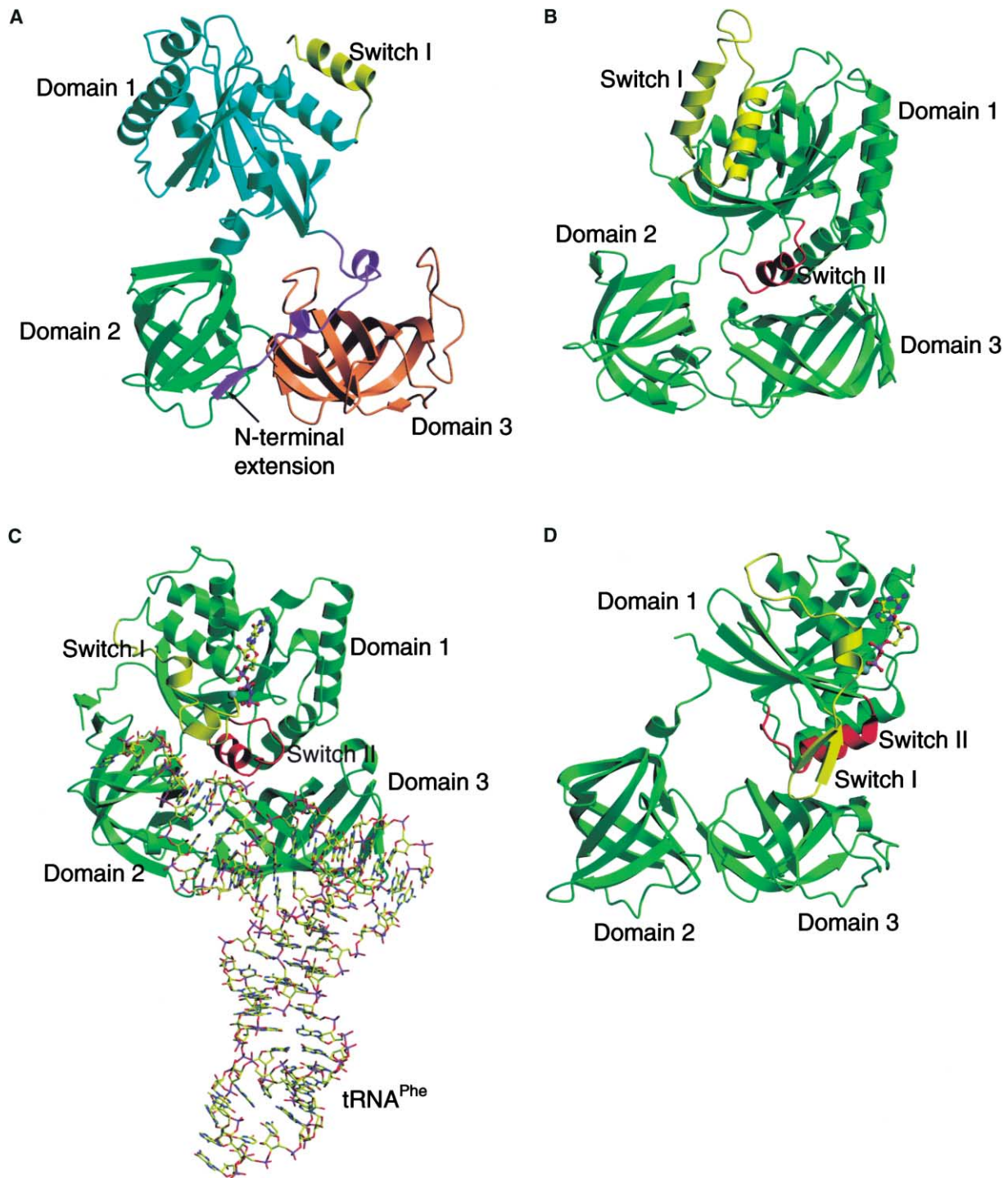


Figure 1. Crystal Structure of eRF3c and Comparison with Other Translational GTPases

The ribbon diagrams are drawn with domains 2 and 3 in the same orientation. Domains 1, 2, and 3 and the N-terminal extension of eRF3c are colored as cyan, green, orange, and magenta, respectively. Switch I and II regions are shown in yellow and red, respectively. Bound nucleotide is shown in ball-and-stick model, and  $Mg^{2+}$  ion in gray sphere. (A) eRF3c. (B) eEF1 $\alpha$  in the eEF1 $\alpha$ -eEF1 $\beta$  complex. (C) EF-Tu-GTP-tRNA complex. (D) EF-Tu-GDP.

activity of SseF1 $\alpha$  (Vitagliano et al., 2001), prompted us to probe the role of  $Mg^{2+}$  in nucleotide binding and exchange in eRF3c. The affinity of eRF3c for GDP or GDPNP in the presence or absence of  $Mg^{2+}$  was mea-

sured using isothermal titration calorimetry (ITC). Surprisingly, whereas no binding of GDP to eRF3c was detected in the presence of 2 mM  $Mg^{2+}$ , eRF3c bound GDP strongly ( $K_d = 3.8 \mu M$ ) in the absence of  $Mg^{2+}$ .

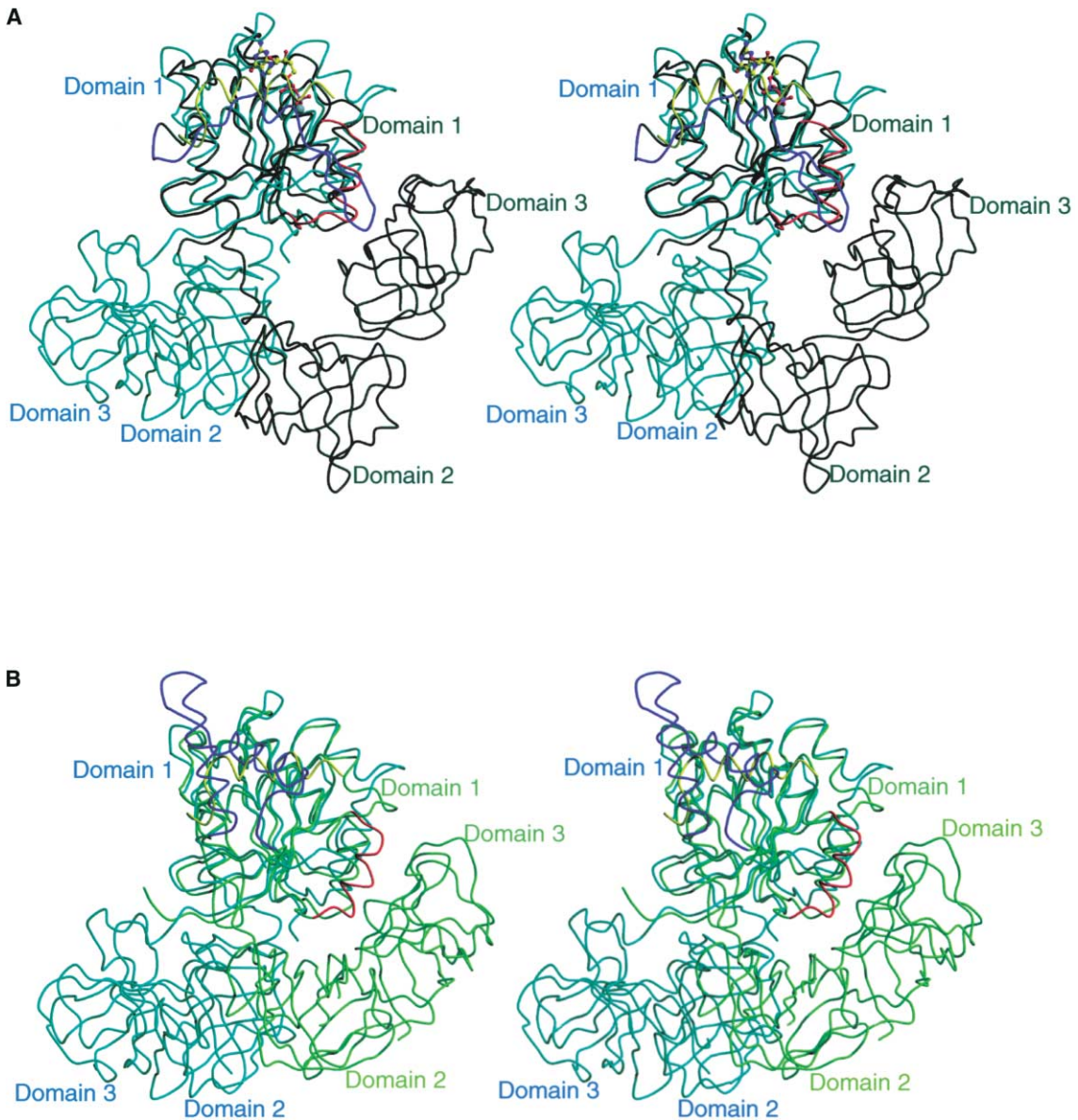


Figure 2. Comparison of eRF3c with EF-Tu-GDP and eEF1 $\alpha$

eRF3c is shown in cyan, EF-Tu-GDP in dark green, and eEF1 $\alpha$  in yellow green. Switch I of eRF3c is shown in yellow while Switch I and II regions in both EF-Tu-GDP and eEF1 $\alpha$  are shown in blue and red, respectively. GDP molecule in EF-Tu-GDP is shown in ball-and-stick model and Mg<sup>2+</sup> ion in gray sphere. (A) Stereo view of superposition of domain 1 of eRF3c with that of EF-Tu-GDP. (B) Stereo view of superposition of domain 1 of eRF3c with that of eEF1 $\alpha$ .

Even at a Mg<sup>2+</sup> concentration as low as 0.3 mM, the affinity of eRF3c for GDP was severely ablated (data not shown). eRF3c bound GDPNP weakly in the absence of Mg<sup>2+</sup> ( $K_d = 200\text{--}300 \mu\text{M}$ ). However, addition of 2 mM Mg<sup>2+</sup> improved the affinity of eRF3c for GDPNP by 2-fold ( $K_d = 100\text{--}150 \mu\text{M}$ ). These observations are in marked contrast to the findings that Mg<sup>2+</sup> is essential for high-affinity binding of guanine nucleotides to the eubacterial elongation factors (Rutthard et al., 2001), and may have important functional implications. The different role Mg<sup>2+</sup> plays in eRF3, EF-Tu, and SseEF1 $\alpha$  is somewhat surprising since the residues of EF-Tu that coordinate Mg<sup>2+</sup> are conserved in eRF3 (Figure 3B), SseEF1 $\alpha$ , and

all the other known eukaryotic EF1 $\alpha$  (Vitagliano et al., 2001). A guanine exchange factor (GEF) is required to catalyze the switch from the GDP to GTP form in G-proteins. However, to date no GEF has been identified for eRF3, and it has been proposed that either a domain in eRF3 or the C-terminal domain of eRF1 act as the GEF to catalyze guanine nucleotide exchange in eRF3 (Kisselev and Buckingham, 2000). In prokaryotes, the ribosome-RF1/RF2 complex functions as a GEF for RF3 (Zavialov et al., 2001). The dissociation of GDP from most G-proteins is greatly inhibited by Mg<sup>2+</sup>, a property exploited by GEFs to mediate nucleotide exchange. Structures of G protein-GEF complexes show that the

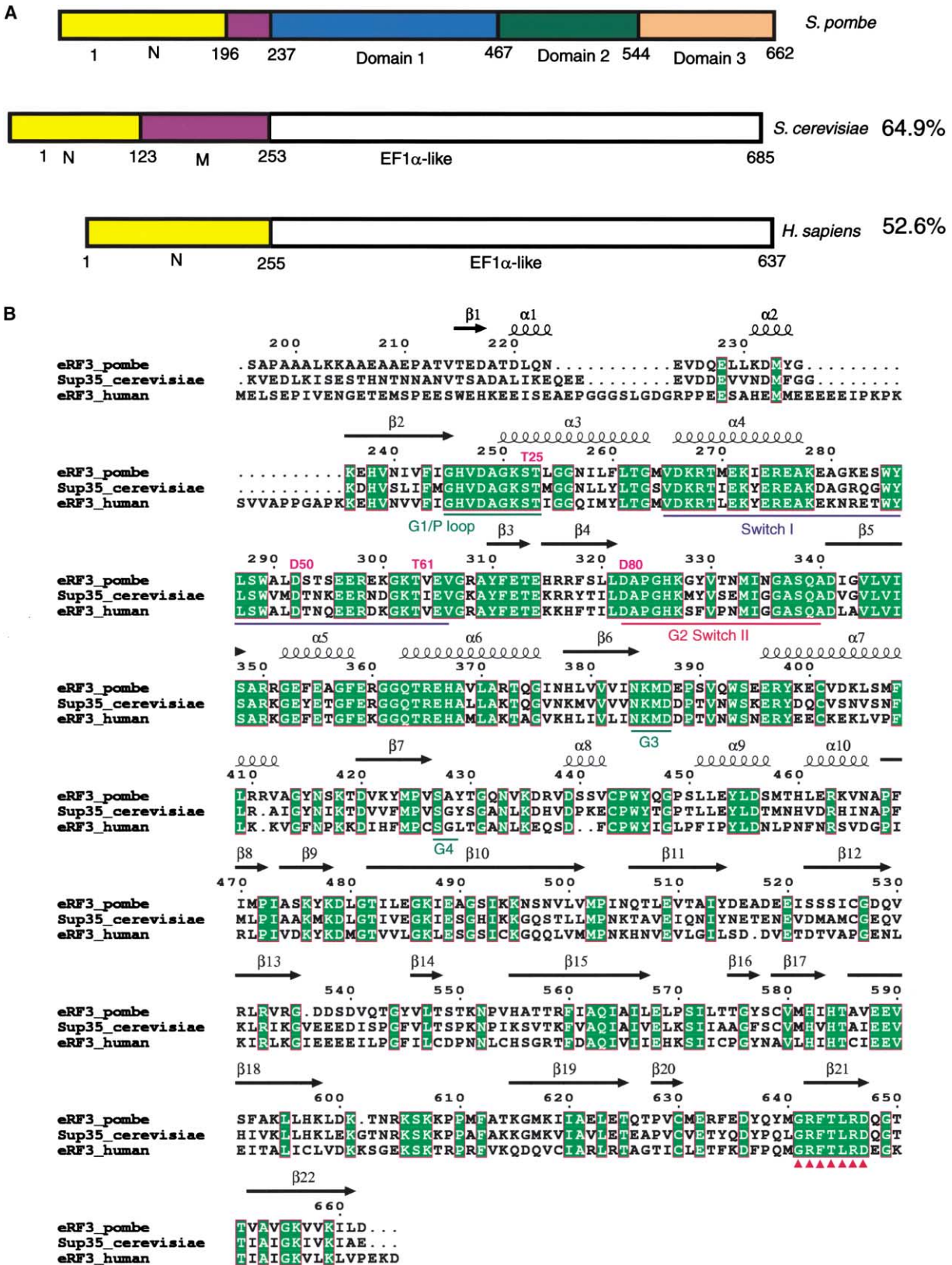


Figure 3. Domain Organization and Sequence Alignments of Selected eRF3 Proteins

(A) Schematic representation of the domain organization of eRF3 proteins from *S. pombe*, *S. cerevisiae*, and *H. sapiens*. The percentages show the sequence similarity of *S. cerevisiae* and *H. sapiens* eRF3 proteins to *S. pombe* protein. The sequence similarity of *S. pombe* eRF3 to *E. coli* RF3 is 17.1%. The coloring scheme for the N-terminal extension, domains 1, 2, and 3 of eRF3 is as in Figure 1A.

(B) Multiple sequence alignment of *S. pombe*, *S. cerevisiae*, and *H. sapiens* eRF3. Invariant residues are colored in green. Secondary structure elements of eRF3c are indicated. GTP binding motifs (G1, G2, G3, and G4) and Switch I and II regions are marked. The GRFTLRD motif is denoted with red arrows. The residues coordinating  $Mg^{2+}$  in *E. coli* EF-Tu are shown in magenta and on top of their *S. pombe* counterparts.

GEF destroys the  $Mg^{2+}$  binding site in the G protein by displacing the switch II region (Cherfils and Chardin, 1999). Our observations that  $Mg^{2+}$  is absent from the GDP binding site of eRF3c, and at higher concentration promotes GDP release, suggests that the first step of nucleotide exchange in eRF3 is the release of the phosphate moiety prompted by  $Mg^{2+}$  binding rather than its removal. The intracellular  $Mg^{2+}$  concentration is  $\sim 0.5$  mM in mammalian cells (Alberts et al., 2002) and  $\sim 0.9$  mM in *S. pombe* (Zhang et al., 1997). At such physiological  $Mg^{2+}$  concentrations, eRF3 would have negligible, if any, affinity for GDP, implying that the GDP to GTP transition of eRF3 would not necessarily require a GEF. On GTP hydrolysis, GDP probably dissociates spontaneously, a notion that could account for the absence of a GEF for eRF3 proteins. Since the concentration of GTP is much higher than that of GDP in the cells, GTP binds to the unoccupied eRF3 upon removal of GDP.

In G-proteins, the rate of GTP hydrolysis is determined either by its intrinsic GTPase activity or by an associated GTPase activating protein (GAP). The extremely low intrinsic GTPase activity of eRF3 is strongly stimulated by the synergistic action of eRF1 and the ribosome (Frolova et al., 1996). This low intrinsic GTPase activity of eRF3 is consistent with our observation that  $Mg^{2+}$  is absent from the eRF3c-GTP crystal structure (Figure 4A), as  $Mg^{2+}$  is essential for GTP hydrolysis (Kjeldgaard et al., 1996). Moreover, our ITC data showed that free eRF3c binds GTP in the absence of  $Mg^{2+}$ , although with lower affinity. It has been proposed that eRF1 in complex with the ribosome may act as a GAP toward eRF3 (Kisselev et al., 2003). The switch II regions of both Ras and RhoA are stabilized by their respective GAPs (for review see Vetter and Wittinghofer, 2001). It is tempting to speculate that switch I and II of eRF3 may become ordered when the eRF1/eRF3-GTP complex associates with the ribosome, thereby stimulating the GTPase activity of eRF3 in the presence of  $Mg^{2+}$ .

#### Interaction of eRF3 with eRF1

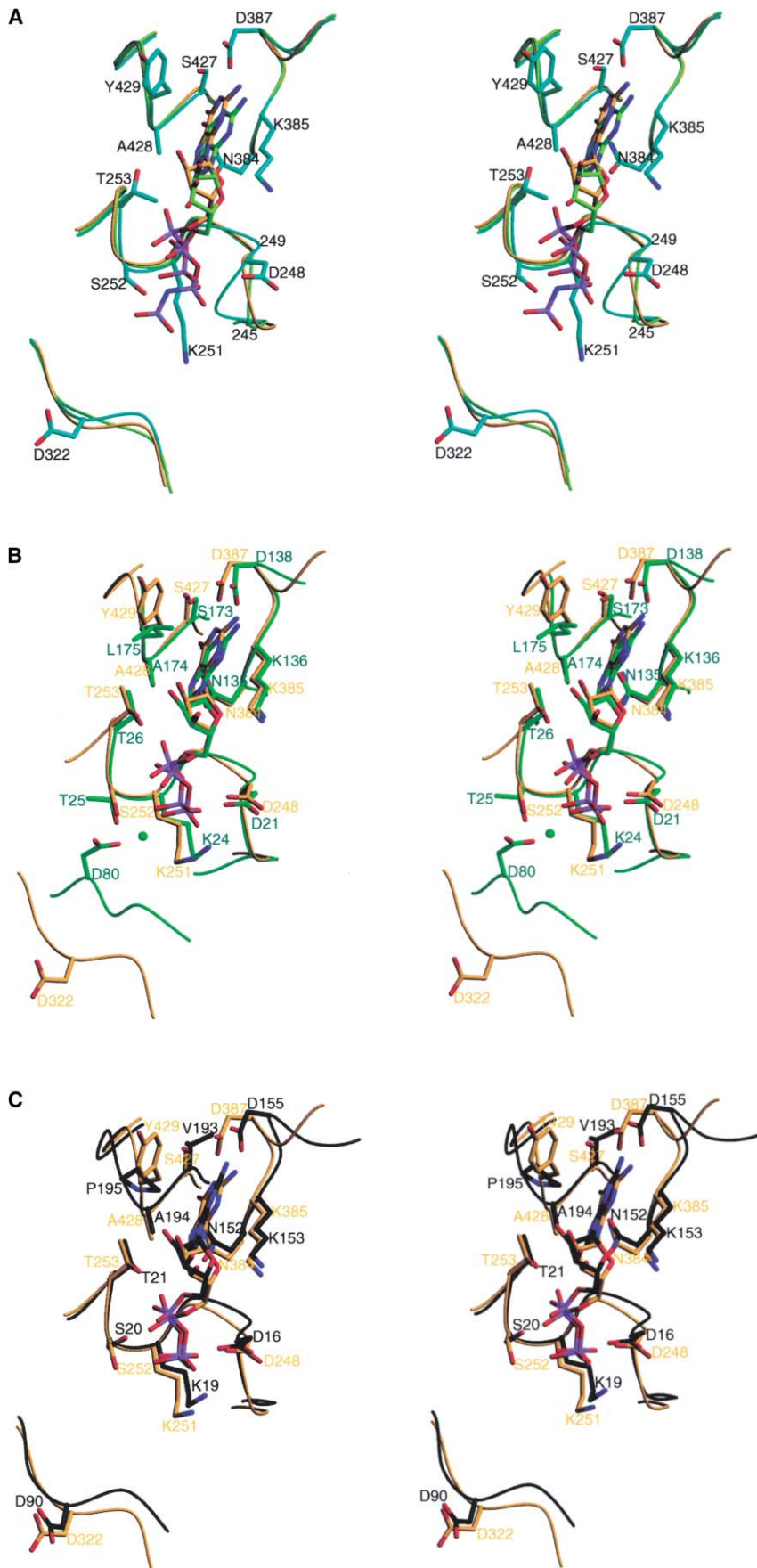
Previous studies demonstrated that eRF1 and eRF3 interact via their respective C-terminal regions (residues 277-433 and 482-662 of *S. pombe* eRF1 and eRF3, respectively) (Ito et al., 1998; Eurwilaichitr et al., 1999; Merkulova et al., 1999; Ebihara and Nakamura, 1999). To provide insight into the eRF1 binding site on eRF3, we mapped the sequence conservation shared by eukaryotic eRF3 proteins on the molecular surface of our fission yeast eRF3c structure. When the nonconserved N-terminal tail (residues 215-236) is included in the surface calculation, a conserved patch, large enough to be a potential eRF1 binding site, is not detectable (Figure 5A). As the interaction between eRF1 and eRF3 does not depend on the N-terminal domains, we removed the N-terminal tail (residues 215-236) and reevaluated the regions of structural conservation. The results clearly showed a prominent conserved patch on domain 3 situated close to the interface between domains 2 and 3 (Figure 5B). This region may represent a potential binding site for eRF1, a notion supported by several observations. First, this region is analogous to the site of domain 3 of EF-Tu that contacts the tRNA stem in the EF-Tu/tRNA/GTP ternary complex (Figure 1C). Domain 3

of eRF1 has been proposed to structurally and functionally mimic the T stem of tRNA molecule (Song et al., 2000). Second, an evolutionally conserved sequence motif GRFTLRD (Figure 3B; residues 641 to 647) in domain 3 of eRF3 is located in this conserved patch, and this motif could play an indispensable role in eRF1 binding (Figures 5B and 5D). Third, in both *S. cerevisiae* and *S. pombe* eRF1, a stretch of extreme C-terminal peptide that is rich in acidic amino acids, has been found to be a primary binding site for eRF3 (Eurwilaichitr, et al., 1999; Ito et al., 1998). Residues 215-236 of eRF3 are abundant in acidic amino acids (Figure 5C) and bind to this region in the eRF3c structure. In the absence of eRF1, residues 215-236 could probably replace the C-terminal tail of eRF1 and occupy the potential eRF1 binding site on the domain 3 of eRF3.

#### The Role of the N-Terminal Extension and the GRFTLRD Motif

To examine the role the N-terminal and the C-terminal regions of eRF3, including the GRFTLRD sequence motif, play in mediating interactions to eRF1, eRF3 variants were created by site-directed mutagenesis and deletion mutant construction. The resulting variant eRF3 proteins were examined for their activity to restore cell growth (i.e., complementation test) and ability to bind to eRF1 (i.e., two-hybrid assay) *in vivo*. In the former assay, variant eRF3 proteins were expressed from the relatively weak CYC promoter in a temperature-sensitive (Ts) lethal *S. cerevisiae* strain (YK21-02, *gst1-1*; Kikuchi et al., 1988) and complementation was monitored by cell growth at the Ts lethal temperature of 37°C. Note that eRF1 and eRF3 are functionally exchangeable between *S. cerevisiae* and *S. pombe* since viability of Ts and knockout mutants of *sup35* and *sup45* of *S. cerevisiae* can be perfectly restored by the *pombe* counterparts (Ito et al., 1998; Ebihara and Nakamura, 1999). The latter assay used a GAL4-based two-hybrid system (Fields and Song, 1989). An N-terminal truncated form of eRF1 (i.e., eRF1- $\Delta$ N2) with efficient binding capacity for eRF3 (Ito et al., 1998) and variant eRF3 polypeptides (this study) were cloned in-frame downstream of the GAL4 activation (AD, plasmid pGBT9) and binding (BD, plasmid pGBKT7) domains, respectively. The resulting plasmids were transformed into *S. cerevisiae* host strain AH109 (CLONTECH Laboratories, Inc. [James et al., 1996]). The AH109 yeast strain contained reporter genes, *HIS3* and *ADE2*, under the control of GAL4-responsive elements, and an *in vivo* protein-protein interaction enabled the reporter transformant to grow on histidine-free and adenine-free minimal medium (SC-His-Ade). The results are shown in Figure 5E showing *S. cerevisiae* growth under restrictive conditions and summarized in Table 2.

When individual N-terminal residues—Thr215, Asp217, Glu228, and Tyr234—of eRF3 were changed to Ala, no significant defects were observed either in restoring the growth of YK21-02 (*gst1-1*) at 37°C or in binding to eRF1- $\Delta$ N2 as monitored by growth on SC-His-Ade (Figure 5E). While an Ala substitution for Met233 was unable to restore the growth of YK21-02, it did not affect the binding to eRF1. The observed adenine prototrophy in the two-hybrid assay was further confirmed in sensitive con-



ditions, in which any reduction in the *ADE2* expression would be reported by the appearance of pink or red colonies on SC-His medium supplemented with low adenine due to the accumulation of metabolic byproducts. However, colonies in this test remained white for all the N-terminal variants of eRF3 (data not shown). The AH109 strain carries another two-hybrid reporter gene, *MEL1*, which produces  $\alpha$ -galactosidase (Aho et al., 1997). The  $\alpha$ -galactosidase is a secreted enzyme and thereby sensitive to monitor *MEL1* expression with colony color on SC-His-Ade plate supplemented with X $\alpha$ Gal. Again, this assay confirmed the above finding that all of the N-terminal variants of eRF3 remained active to interact with eRF1 in vivo (data not shown). Although the N-terminal deletion up to position 232 ( $\Delta$ N2) apparently abolished eRF3 function under these conditions, this was due to the decreased protein's stability rather than any decrease in protein activity (data not shown). These results indicate that all the alterations examined in the N-terminal extension with rich acidic amino acids do not interfere with binding to eRF1 although the same region is shown structurally to bind to the potential eRF1 binding site (Figure 5D). This, nevertheless, should not exclude the possibility that the N-terminal extension is able to repress or modulate eRF1 binding to eRF3 in a competitive manner under certain physiological conditions.

In contrast to the N-terminal variants, the C-terminal changes exhibited remarkable defects in cell growth and binding to eRF1. Mutations that result in apparent defects are classified into two groups. The first group shows reduced viability and reduced interaction with eRF1, while the second group shows reduced viability yet no reduced ability to interact with eRF1. The first group includes substitutions for Phe643 and Arg646 as well as C-terminal truncations beyond Lys656 ( $\Delta$ C1), and the second group includes substitutions for His582, Arg642, Val654, and Lys656 (Figures 5D and 5E; Table 2). Mutational changes at the other positions tested, Thr585, Phe634, and Tyr639, did not show any apparent defects. These findings point out two important conclusions. First, a prominent conserved patch on domain 3, which includes Phe643 and Arg646, plays a crucial role for binding to eRF1 although other residues in this patch may not necessarily be directly involved in the binding. Second, the C-terminal of eRF3, which includes His582, Arg642, Val654, and Lys656, is vital for the essential functions other than interacting with eRF1. Therefore, although two Arg residues, Arg642 and Arg646, are conserved in the predicted patch, it is likely that they have different roles in eRF3 function. It is also noteworthy that when His582 and Arg646 are doubly mutated, loss of viability is enhanced while loss of binding with eRF1

remains the same as the single mutant Arg646 $\rightarrow$ Ala (Figure 5E; Table 2). This again reinforces the involvement of a vital, yet unidentified, function for the C-terminal of eRF3. Consistent with this notion, depletion of yeast eRF3 not only enhanced the nonsense suppression but also caused various defects in cytoskeleton organization and cell cycle regulation (Valouev et al., 2002). The C-terminal eEF1 $\alpha$ -like region of eRF3 has been shown to be responsible for these defects. However, whether the C-terminal tail of eRF3 is culprit for such defects remains to be examined.

## Conclusions

The structures of eRF3c in three distinct functional states presented here revealed that the eRF3c is similar to EF-Tu, supporting the findings that RF3 and EF-Tu have similar modes of action (Zavialov et al., 2001). Our results also strengthen the notion that the mechanism of translation termination in prokaryotes and eukaryotes may indeed be similar. We have shown that Mg<sup>2+</sup> is absent from the nucleotide binding site of eRF3c due to associated conformational change and disorder of three essential residues that are required to coordinate Mg<sup>2+</sup>. The structure of eRF3c reveals features of the nucleotide binding that are similar to those observed in the structure of SsEF1 $\alpha$  (Vitagliano et al., 2001). Our observation that Mg<sup>2+</sup> (>0.3 mM) weakens the GDP binding substantially but strengthens GTP binding in solution implies that intracellular Mg<sup>2+</sup> would effectively prevent GDP binding to eRF3, and at the same time promote GTP binding to eRF3. Such a novel nucleotide exchange mechanism argues in favor of the absence of a GEF for eukaryotic eRF3 proteins, although the possibility that the ribosome together with eRF1 act as a GEF for eRF3 cannot be excluded. The failure of both Mg<sup>2+</sup>/GTP and Mg<sup>2+</sup>/GDP to promote structural changes in the switch I and switch II regions of eRF3 was unexpected. It is possible that although switch I and II do not participate in crystal lattice contacts, tertiary conformational changes within eRF3, associated with guanine nucleotide engagement, were prevented by crystal packing forces. Alternatively, as suggested above, switch I and switch II may adopt active conformations only in the presence of eRF1 and the ribosome.

Mapping sequence conservation shared by the eukaryotic eRF3 proteins on the molecular surface of eRF3c reveals a prominent region consisting of the evolutionally conserved GRFTLRD motif, as a potential eRF1 binding site. Mutagenesis experiments demonstrated the importance of this region and the C-terminal tail in cell viability and eRF1 binding. The N-terminal

Figure 4. Comparison of the Nucleotide Binding Sites of eRF3c with EF-Tu-GDP and SsEF1 $\alpha$

The GDP/GDPNP molecule, and the residues involved in interactions with GDP/GDPNP or Mg<sup>2+</sup> coordination, are shown in stick models. Mg<sup>2+</sup> ion is shown as a green sphere in EF-Tu-GDP.

(A) Stereo view of superposition of the GDP binding sites of apo-eRF3c, eRF3c-GDP, and eRF3c-GTP. eRF3c, eRF3c-GDP, and eRF3c-GTP are shown in cyan, orange, and yellow green, respectively. For clarity, only residues from apo-eRF3c are shown. The positions of residues 245 and 249 are marked.

(B) Stereo view of superposition of the GDP binding sites of eRF3c-GDP and EF-Tu-GDP. eRF3c-GDP is colored as in (A) and EF-Tu-GDP in green. Residues from eRF3c-GDP and EF-Tu-GDP are labeled in orange and green, respectively.

(C) Stereo view of superposition of the GDP binding sites of eRF3c-GDP and SsEF1 $\alpha$ . eRF3c-GDP is colored as in (A) while SsEF1 $\alpha$  in black. Residues from eRF3c-GDP and SsEF1 $\alpha$  are labeled in orange and black, respectively.



Table 2. Complementation and eRF1-Binding Activity of N-Terminal and C-Terminal Variants of eRF3

Alterations in eRF3	Complementation of <i>sup35</i> (ts) Allele <sup>a</sup>	eRF1 Binding <sup>b</sup>
Empty vector	–	–
Wild-type	+++	+++
Amino acid substitutions		
E228A	+++	+++
D217A	++	+++
T215A	+++	+++
H582A	+	+++
R646A	+/-	+/-
F643A	+	+/-
R642A	–	+++
T585A	+++	+++
Y234A	+++	+++
M233A	+/-	+++
Y639A	+++	+++
F634A	+++	+++
K656A	+/-	+++
V654A	++	+++
H582A/R646A	–	+/-
N-terminal deletions up to amino acid positions		
218	+++	ND
232 ( $\Delta$ N2)	–	ND
C-terminal deletions up to amino acid positions		
656 ( $\Delta$ C1)	–	–
650	–	ND
647	–	ND
643	–	ND
640	–	ND

<sup>a</sup>YK21-02 (*sup35* ts; Kikuchi et al., 1988) strain was transformed with p416CYC carrying the indicated eRF3 variants and the transformants' growth at 37°C was tested as shown in Figure 5E: +++, normal growth (large colony); ++, fair growth (medium colony); +, weak growth (small colony); +/-, sick growth (tiny colony); –, no growth.

<sup>b</sup>The binding activity of eRF3 variants (cloned in pGBKT7, BD plasmid) to eRF1- $\Delta$ N2 (cloned in pGBT9, AD plasmid) was monitored by growth of AH109 transformants on SC-His-Ade as shown in Figure 5E: +++ (strong binding); + (weak binding); +/- (very weak binding if any); – (no binding). ND, no data.

extension binds to the potential eRF1 binding site, possibly regulating eRF1 binding in a competitive manner.

#### Experimental Procedures

##### Protein Purification

The cDNA encoding a truncated eRF3 (eRF3c; residues 196-662) was cloned from *S. pombe* genomic DNA, and expressed as a GST-fusion protein in *E. coli*. The protein was purified using Glutathione Sepharose 4B, Mono S cation exchange, and Superdex 75 gel filtration columns (Amersham Biosciences). The protein was concentrated to ~10 mg/ml for crystallizations. SeMet substituted eRF3c was purified in the same way except that the DTT concentration is 10 mM.

#### Crystallization, Data Collection, and Structure Determination

Crystals of eRF3c were grown at 4°C by hanging drop vapor diffusion. Equal volume of protein solution was mixed with the precipitant solution (100 mM HEPES [pH 7.5], 2%–8% PEG 8,000 (w/v), 12%–18% ethylene glycol (v/v), 10 mM DTT, 5% (v/v) glycerol, and 150 mM NaCl). The crystals of eRF3c-GDP and eRF3c-GTP were obtained by soaking native crystals in a stabilizing buffer containing either 1 mM GDP or GDPNP and 2 mM Mg<sup>2+</sup>. Before data collection, crystals were transferred to the stabilizing solution including 30% (v/v) ethylene glycol and fast frozen in liquid nitrogen.

SeMet MAD data were collected at two wavelengths ( $\lambda$ 1:peak;  $\lambda$ 2:remote) on BM14UK at ESRF (Grenoble, France) using a MarCCD detector and processed with the HKL software package (Otwinowski and Minor, 1997). Crystals belong to space group P4<sub>3</sub>2<sub>1</sub>2, with the cell parameters of a = b = 83.80 Å, c = 165.94 Å with one molecule per asymmetric unit. Data collection of eRF3c-GDP and eRF3c-GTP was carried out at beamline BW7A, EMBL (Hamburg, Germany). Diffraction data were recorded on a MarCCD detector and processed with MOSFLM and CCP4 (CCP4, 1994).

Thirteen out of possible 15 Se site were found using the program SOLVE (Terwilliger and Berendzen, 1999). Heavy atom refinement and phasing were carried out using SHARP (De La Fortelle and Bricogne, 1997). About 70% of the final model was built automatically using ARP/wARP (Perrakis et al., 1999). The rest of the model building was carried out manually using program O (Jones, et al., 1991). Crystallographic refinement was performed with CNS (Brünger, et al., 1998). Water molecules were automatically included with CNS and manually edited with electron densities. The final round of refinement was carried out with REFMAC5 (Murshudov et al., 1997). The structures of eRF3c-GDP and eRF3c-GTP were solved by molecular replacement method using eRF3c as a search model. Crystallographic refinement was carried out with REFMAC5 (Murshudov et al., 1997). The final refinement statistics are summarized in Table 1.

#### Isothermal Titration Calorimetry Assay

Measurement of binding between guanine nucleotides (GDP or GDPNP) and eRF3c was carried out with a Micro Calorimetry System (Microcal, Inc) at 20°C. 20 aliquots of 10  $\mu$ l GDP (500  $\mu$ M) or GDPNP (800  $\mu$ M) were injected into 1.4 ml of eRF3c (30  $\mu$ M and 50  $\mu$ M for GDP and GDPNP titration, respectively) in 20 mM Tris (pH 7.4) containing 150 mM NaCl and either 2 mM EDTA or MgCl<sub>2</sub>. The heat of dilution obtained from injecting a ligand into buffer was subtracted before the K<sub>d</sub> values and the binding ratios were calculated by the ORIGIN data analysis software (Microcal, Inc).

#### Strains, Media, and Plasmids

The yeast strains used are YK21-02 (*MAT $\alpha$*  *ura3* *trp1* *his3* *gst1-1* (ts) affecting *sup35*; Kikuchi et al., 1988) and AH109 (*MAT $\alpha$* , *trp1-901*, *leu2-3*, *112*, *ura3-52*, *his3-200*, *gal4 $\Delta$* , *gal80 $\Delta$* , *LYS2::GAL1<sub>UAS</sub>-GAL1<sub>TATA</sub>-HIS3*, *GAL2<sub>UAS</sub>-GAL2<sub>TATA</sub>-ADE2*, *URA3::MEL1<sub>UAS</sub>-MEL1<sub>TATA</sub>-lacZ*). Yeast cultures were grown using standard conditions in YPD liquid medium (2% w/v Bacto-peptone, 1% w/v yeast extract, and 2% w/v glucose). Yeast transformants were grown in synthetic complete (SC) media supplemented with the required amino acids and cofactors. Yeast plasmids carrying *S. pombe* eRF1 and eRF3 sequences have been described previously (Ito et al., 1998; Ebihara and Nakamura, 1999) and are used for further gene manipulations. eRF3 mutants were generated using Mutan-K site-directed muta-

are labeled including those from the GRFTLRD motif. The coloring scheme is as in (A)

(C) Solvent accessible surface and electrostatic potential of eRF3c with the N-terminal extension included in the surface calculation. The large negative charged patch and the position of the N-terminal extension are marked.

(D) The figure shows the location of the mutated residues listed in Table 2 in eRF3c. The coloring scheme for the domains of eRF3c is as in Figure 1A. The C-terminal tail and the GRFTLRD motif are colored in red and blue, respectively.

(E) The activity of eRF3 variants for yeast viability and binding to eRF1 in vivo. The eRF3 variants carrying the indicated alterations (see Table 2) were cloned into plasmids p416CYC and pGBKT7 for complementation and two-hybrid analyses, respectively. The binding activity of eRF3 variants (cloned in pGBKT7, BD plasmid) to eRF1- $\Delta$ N2 (cloned in pGBT9, AD plasmid) was monitored by growth of the AH109 double transformants on SC-His-Ade. Complementation to restore Sup35 activity was monitored by the growth of YK21-02 (*sup35* ts) transformants at both 30°C and 37°C on SC agar plates. Upper panel, N-terminal variants of eRF3. Lower panel, C-terminal variants of eRF3.

genesis kit (Takara) according to the manufacturer's instructions. The resulting variants and wild-type sequences are cloned into plasmids p416CYC (*ARS CEN URA3*; Mumberg et al., 1995) and pGBKT7 (BD *TRP1*; Louvet et al., 1997) for complementation and two-hybrid assays, respectively. The in vivo two-hybrid assay was carried out by the same procedures and conditions as described previously (Ito et al., 1998).

#### Acknowledgments

We thank Dr. Paul Tucker at BW7A (European Molecular Biology Laboratory, Hamburg, Germany) for assistance and access to synchrotron radiation facilities. This work was supported by grants from the following: the Agency for Science, Technology and Research (A\* Star) in Singapore (to H.S.); The Ministry of Education, Sports, Culture, Science and Technology of Japan (MEXT); and the Organization for Pharmaceutical Safety and Research (OPSR) to Y.N.

Received: January 16, 2004

Revised: March 3, 2004

Accepted: March 10, 2004

Published: April 22, 2004

#### References

- Aho, S., Arffman, A., Pummi, T., and Uitto, J. (1997). A novel reporter gene MEL1 for the yeast two-hybrid system. *Anal. Biochem.* **253**, 270–272.
- Alberts, B., Johnson, A., Lewis, J., Raff, M., Roberts, K., and Walter, P. (2002). *Molecular Biology of The Cell*, Fourth Edition (New York: Garland Science, Taylor & Francis Group Press), pp. 616.
- Andersen, G.R., Pedersen, L., Valente, L., Chatterjee, I., Kinzy, T.G., Kjeldgaard, M., and Nyborg, J. (2000a). Structural basis for nucleotide exchange and competition with tRNA in the yeast elongation factor complex eEF1A:eEF1B $\alpha$ . *Mol. Cell* **6**, 1261–1266.
- Andersen, G.R., Thirup, S., Spemullil, L.L., and Nyborg, J. (2000b). High resolution crystal structure of bovine mitochondrial EF-Tu in complex with GDP. *J. Mol. Biol.* **297**, 421–436.
- Andersen, G.R., Valente, L., Pedersen, L., Kinzy, T.G., and Nyborg, J. (2001). Crystal structures of nucleotide exchange intermediates in the eEF1A-eEF1B $\alpha$  complex. *Nat. Struct. Biol.* **8**, 531–534.
- Berchtold, H., Reshetnikova, L., Reiser, C.O., Schirmer, N.K., Sprinzl, M., and Hilgenfeld, R. (1993). Crystal structure of active elongation factor Tu reveals major domain rearrangements. *Nature* **365**, 126–132.
- Brünger, A.T., Adams, P.D., Clore, G.M., DeLano, W.L., Gros, P., Grosse-Kunstleve, R.W., Jiang, J.S., Kuszewski, J., Nilges, M., Pannu, N.S., et al. (1998). Crystallography and NMR system: a new software suite for macromolecular structure determination. *Acta Crystallogr. D* **54**, 905–921.
- CCP4 (Collaborative Computational Project No.4) (1994). The CCP4 suite: programs for protein crystallography. *Acta Crystallogr. D* **50**, 760–763.
- Cherfils, J., and Chardin, P. (1999). GEFs: structural basis for their activation of small GTP-binding proteins. *Trends Biochem. Sci.* **24**, 306–311.
- Chemoff, Y.O., Uptain, S.M., and Lindquist, S.L. (2002). Analysis of prion factors in yeast. *Methods Enzymol.* **351**, 499–538.
- Czaplinski, K., Ruiz-Echevarria, M.J., Gonzalez, C.I., and Peltz, S.W. (1999). Should we kill the messenger? The role of the surveillance complex in translation termination and mRNA turnover. *Bioessays* **21**, 685–696.
- De La Fortelle, E., and Bricogne, G. (1997). Maximum-likelihood heavy-atom parameter refinement for Multiple Isomorphous Replacement and Multiwavelength Anomalous Diffraction method. *Methods Enzymol.* **276**, 472–494.
- Ebihara, K., and Nakamura, Y. (1999). C-terminal interaction of translational release factors eRF1 and eRF3 of fission yeast: G-domain uncoupled binding and the role of conserved amino acids. *RNA* **5**, 739–750.
- Eurwilaichitr, L., Graves, F.M., Stansfield, I., and Tuite, M.F. (1999). The C-terminus of eRF1 defines a functionally important domain for translation termination in *Saccharomyces cerevisiae*. *Mol. Microbiol.* **32**, 485–496.
- Fields, S., and Song, O. (1989). A novel genetic system to detect protein-protein interactions. *Nature* **340**, 245–246.
- Frolova, L., Le Goff, X., Rasmussen, H.H., Cheperegin, S., Drugeon, G., Kress, M., Arman, I., Haenni, A.-L., Celis, J.E., Philippe, M., et al. (1994). A highly conserved eukaryotic protein family possessing properties of polypeptide chain release factor. *Nature* **372**, 701–703.
- Frolova, L., Le Goff, X., Zhouravleva, G., Davydova, E., Philippe, M., and Kisselev, L. (1996). Eukaryotic polypeptide chain release factor eRF3 is an eRF1- and ribosome-dependent guanosine triphosphatase. *RNA* **2**, 334–341.
- Frolova, L.Y., Merkulova, T.I., and Kisselev, L. (2000). Translation termination in eukaryotes: polypeptide release factor eRF1 is composed of functionally and structurally distinct domains. *RNA* **6**, 381–390.
- Hoshino, S., Miyazawa, H., Enomoto, T., Hanaoka, F., Kikuchi, Y., Kikuchi, A., and Ui, M. (1989). A human homologue of the yeast *GST1* gene codes for a GTP-binding protein and is expressed in a proliferation-dependent manner in mammalian cells. *EMBO J.* **8**, 3807–3814.
- Hoshino, S., Imai, M., Mizutani, M., Kikuchi, Y., Hanaoka, F., Ui, M., and Katada, T. (1998). Molecular cloning of a novel member of the eukaryotic polypeptide chain-releasing factors (eRF). Its identification as eRF3 interacting with eRF1. *J. Biol. Chem.* **273**, 22254–22259.
- Hoshino, S., Imai, M., Kobayashi, T., Uchida, N., and Katada, T. (1999). The eukaryotic polypeptide chain releasing factor (eRF3/GSPT) carrying the translation termination signal to the 3'-poly(A) tail of mRNA. Direct association of eRF3/GSPT with polyadenylate-binding protein. *J. Biol. Chem.* **274**, 16677–16680.
- Inge-Vechtomov, S., Zhouravleva, G., and Philippe, M. (2003). Eukaryotic release factors (eRFs) history. *Biol. Cell.* **95**, 195–209.
- Ito, K., Ebihara, K., and Nakamura, Y. (1998). The stretch of C-terminal acidic amino acids of translational release factor eRF1 is a primary binding site for eRF3 of fission yeast. *RNA* **4**, 958–972.
- James, P., Halladay, J., and Craig, E.A. (1996). Genomic libraries and a host strain designed for highly efficient two-hybrid selection in yeast. *Genetics* **144**, 1425–1436.
- Jones, T.A., Zou, J.Y., Cowan, S.W., and Kjeldgaard, M. (1991). Improved methods for building protein models in electron density maps and the location of errors in these models. *Acta Crystallogr. A* **47**, 110–119.
- Kikuchi, Y., Shimatake, H., and Kikuchi, A. (1988). A yeast gene required for the G1-to-S transition encodes a protein containing an A-kinase target site and GTPase domain. *EMBO J.* **7**, 1175–1182.
- Kisselev, L., and Buckingham, R.H. (2000). Translation termination comes of age. *Trends Biochem. Sci.* **25**, 561–566.
- Kisselev, L., Ehrenberg, M., and Frolova, L. (2003). Termination of translation: interplay of mRNA, rRNAs and release factors? *EMBO J.* **22**, 175–182.
- Kjeldgaard, M., and Nyborg, J. (1992). Refined structure of elongation factor EF-Tu from *Escherichia coli*. *J. Mol. Biol.* **223**, 721–742.
- Kjeldgaard, M., Nyborg, J., and Clark, B.F. (1996). The GTP binding motif: variations on a theme. *FASEB J.* **10**, 1347–1368.
- Klaholz, B.P., Pape, T., Zavialov, A.V., Myasnikov, A.G., Orlova, E.V., Vestergaard, B., Ehrenberg, M., and van Heel, M. (2003). Structure of the *Escherichia coli* ribosomal termination complex with release factor 2. *Nature* **421**, 90–94.
- Louvet, O., Doignon, F., and Crouzet, M. (1997). Stable DNA-binding yeast vector allowing high-bait expression for use in the two-hybrid system. *Biotechniques* **23**, 816–820.
- Merkulova, T.I., Frolova, L.Y., Lazar, M., Camonis, J., and Kisselev, L. (1999). C-terminal domains of human translation termination factors eRF1 and eRF3 mediate their in vivo interaction. *FEBS Lett.* **443**, 41–47.
- Mumberg, D., Müller, R., and Funk, M. (1995). Yeast vectors for the

- controlled expression of heterologous proteins in different genetic backgrounds. *Gene* 156, 119–122.
- Murshudov, G.N., Vagin, A.A., and Dodson, E.J. (1997). Refinement of macromolecular structures by the maximum-likelihood method. *Acta Crystallogr. D* 53, 240–255.
- Nakamura, Y., and Ito, K. (2003). Making sense of mimic in translation termination. *Trends Biochem. Sci.* 28, 99–105.
- Nakamura, Y., Ito, K., and Ehrenberg, M. (2000). Mimicry grasps reality in translation termination. *Cell* 101, 349–352.
- Nissen, P., Kjeldgaard, M., Thirup, S., Polekhina, G., Reshetnikova, L., Clark, B., and Nyborg, J. (1995). Crystal structure of the ternary complex of Phe-tRNA<sup>Phe</sup>, EF-Tu, and a GTP analog. *Science* 270, 1464–1472.
- Otwinowski, Z., and Minor, W. (1997). Processing of X-ray diffraction data collected in oscillation mode. *Methods Enzymol.* 276, 307–326.
- Perrakis, A., Morris, R., and Lamzin, V.S. (1999). Automated protein model building combined with iterative structure refinement. *Nat. Struct. Biol.* 6, 458–463.
- Rawat, U.B., Zavalov, A.V., Sengupta, J., Valle, M., Grassucci, R.A., Linde, J., Vestergaard, B., Ehrenberg, M., and Frank, J. (2003). A cryo-electron microscopic study of ribosome-bound termination factor RF2. *Nature* 421, 87–90.
- Rutthard, H., Banerjee, A., and Makinen, M.W. (2001). Mg<sup>2+</sup> is not catalytically required in the intrinsic and kirromycin-stimulated GTPase action of *Thermus thermophilus* EF-Tu. *J. Biol. Chem.* 276, 18728–18733.
- Serio, T.R., and Lindquist, S.L. (2000). Protein-only inheritance in yeast: something to get [PSI<sup>+</sup>]-ched about. *Trends Cell Biol.* 10, 98–105.
- Song, H., Parsons, M.R., Rowsell, S., Leonard, G., and Phillips, S.E. (1999). Crystal structure of intact elongation factor EF-Tu from *Escherichia coli* in GDP conformation at 2.05 Å resolution. *J. Mol. Biol.* 285, 1245–1256.
- Song, H., Mugnier, P., Das, A.K., Webb, H.M., Evans, D.R., Tuite, M.F., Hemmings, B.A., and Barford, D. (2000). The crystal structure of human eukaryotic release factor eRF1-mechanism of stop codon recognition and peptidyl-tRNA hydrolysis. *Cell* 100, 311–321.
- Stansfield, I., Jones, K.M., Kushnirov, V.V., Dagkesamanskaya, A.R., Poznyakovski, A.I., Paushkin, S.V., Nierras, C.R., Cox, B.S., Ter-Avanesyan, M.D., and Tuite, M.F. (1995). The product of the SUP45 (eRF1) and SUP35 genes interact to mediate translation termination in *Saccharomyces cerevisiae*. *EMBO J.* 14, 4365–4373.
- Ter-Avanesyan, M.D., Kushnirov, V.V., Dagkesamanskaya, A.R., Didichenko, S.A., Chernoff, Y.O., Inge-Vechtomo, S.G., and Smirnov, V.N. (1993). Deletion analysis of the SUP35 gene of the yeast *Saccharomyces cerevisiae* reveals two non-overlapping functional regions in the encoded protein. *Mol. Microbiol.* 7, 683–692.
- Terwilliger, T.C., and Berendzen, J. (1999). Automated MAD and MIR structure solution. *Acta Crystallogr. D* 55, 849–861.
- Uchida, N., Hoshino, S., Imataka, H., Sonenberg, N., and Katada, T. (2002). A novel role of the mammalian GSPT/eRF3 associating with poly(A)-binding protein in cap/poly(A)-dependent translation. *J. Biol. Chem.* 277, 50286–50292.
- Valouev, I.A., Kushnirov, V.V., and Ter-Avanesyan, M.D. (2002). Yeast polypeptide chain release factors eRF1 and eRF3 are involved in cytoskeleton organization and cell cycle regulation. *Cell Motil. Cytoskeleton* 52, 161–173.
- Vestergaard, B., Van, L.B., Andersen, G.R., Nyborg, J., Buckingham, R.H., and Kjeldgaard, M. (2001). Bacterial polypeptide release factor RF2 is structurally distinct from eukaryotic eRF1. *Mol. Cell* 8, 1375–1382.
- Vetter, I.R., and Wittinghofer, A. (2001). The guanine nucleotide-binding switch in three dimensions. *Science* 294, 1299–1304.
- Vitagliano, L., Masullo, M., Sica, F., Zagari, A., and Bocchini, V. (2001). The crystal structure of *Sulfolobus solfataricus* elongation factor 1 $\alpha$  in complex with GDP reveals novel features in nucleotide binding and exchange. *EMBO J.* 20, 5305–5311.
- Wang, W., Czaplinski, K., Rao, Y., and Peltz, S.W. (2001). The role of Upf proteins in modulating the translation read-through of non-sense-containing transcripts. *EMBO J.* 20, 880–890.
- Zavalov, A.V., Buckingham, R.H., and Ehrenberg, M. (2001). A post-termination ribosomal complex is the guanine nucleotide exchange factor for peptide release factor RF3. *Cell* 107, 115–124.
- Zhang, A., Cheng, T.P., Wu, X.Y., Aitara, B.T., and Altura, B.M. (1997). Extracellular Mg<sup>2+</sup> regulates intracellular Mg<sup>2+</sup> and its subcellular compartmentation in fission yeast, *Schizosaccharomyces pombe*. *Cell. Mol. Life Sci.* 53, 69–72.
- Zhouravleva, G., Frolova, L., Le Goff, X., Le Guellec, R., Inge-Vechtomo, S., Kisselev, L., and Philippe, M. (1995). Termination of translation in eukaryotes is governed by two interacting polypeptide chain release factors, eRF1 and eRF3. *EMBO J.* 14, 4065–4072.

#### Accession Numbers

The coordinates and structure-factor amplitudes of eRF3c, eRF3c-GDP, and eRF3c-GTP have been deposited in the Protein Data Bank with accession codes 1R5B, 1R5N, and 1R5O, respectively.